May 1999

An Idea for Electromagnetic "Feedforward-Feedbackward" Media

Charles Anthony Moses
University of Pennsylvania

Nader Engheta
University of Pennsylvania, engheta@ee.upenn.edu

Follow this and additional works at: http://repository.upenn.edu/ese_papers

An Idea for Electromagnetic "Feedforward-Feedbackward" Media

Abstract

In this paper, an idea for a new class of complex media that we name feedforward–feedbackward (FFFB) media is presented and some of the results of our theoretical work in analyzing plane wave propagation in the axial direction through these media are described. The concept of FFFB media, as introduced here, was inspired by the theoretical research of Saadoun and Engheta on a variation of artificial chiral media. Like chiral media, to our knowledge there are no *naturally occurring* FFFB media for the *microwave* frequency band; for this reason we introduce an idea for artificial FFFB media. The focus of this paper is on one conceptualization of such media, namely dipole–dipole FFFB media. First, we present the calculation of the necessary constitutive parameters for studying axial plane wave propagation. Then we solve the macroscopic Maxwell equations in the k domain for axial plane wave propagation in an unbounded source-free crossed-dipole FFFB medium. Finally, we present the dispersion equation for this medium in this case, discuss some of the physical properties of its roots and certain features of the polarization eigenstates, and briefly speculate some of the potential applications of this medium.

An Idea for Electromagnetic "Feedforward–Feedbackward" Media

Charles A. Moses, *Member, IEEE*, and Nader Engheta, *Fellow, IEEE*

Abstract— In this paper, an idea for a new class of complex media that we name feedforward–feedbackward (FFFB) media is presented and some of the results of our theoretical work in analyzing plane wave propagation in the axial direction through these media are described. The concept of FFFB media, as introduced here, was inspired by the theoretical research of Saadoun and Engheta on a variation of artificial chiral media. Like chiral media, to our knowledge there are no *naturally occurring* FFFB media for the *microwave* frequency band; for this reason we introduce an idea for artificial FFFB media. The focus of this paper is on one conceptualization of such media, namely dipole–dipole FFFB media. First, we present the calculation of the necessary constitutive parameters for studying axial plane wave propagation. Then we solve the macroscopic Maxwell equations in the k domain for axial plane wave propagation in an unbounded source-free crossed-dipole FFFB medium. Finally, we present the dispersion equation for this medium in this case, discuss some of the physical properties of its roots and certain features of the polarization eigenstates, and briefly speculate some of the potential applications of this medium.

Index Terms— Artificial media, complex media, FFFB media, plane wave propagation.

I. INTRODUCTION

AS put by Lindell *et al.* [1, p. 193], "No real media are homogeneous"—at some scale materials always exhibit inhomogeneity. Real dielectrics are necessarily inhomogeneous with properties varying rapidly as a function of position according to the microscopic atomic structure of the dielectric. Certain features, such as anisotropy, temporal dispersion, spatial dispersion, and chirality, which are all observed at optical wavelengths, arise from the microscopic structure of the atoms or molecules comprising the material. Some of these features may be difficult to observe outside of the optical band; at lower frequencies the period of oscillation may be much longer than the atomic relaxation time constant, effectively "washing out" the effects of retardation. At higher frequencies, Bragg diffraction may be prevalent and the geometrical structure of the lattice is emphasized rather than the average properties of the medium. Many materials do exhibit similar features at suboptical frequencies as at optical frequencies, so devices such as lenses, polarizers, or filters at these frequencies can be designed to behave like their optical counterparts by a simple length scaling of all dimensions; however, as a result of the increased volume but more or less constant material density,

the excessive bulk and weight of such devices relegate them unattractive for practical use [2, p. 749].

Artificial materials (also known as artificial dielectrics and complex media) attempt to produce optical effects at suboptical frequencies by more attractive means. An artificial material is a composite medium consisting of a number of closely spaced inclusions distributed throughout some host medium; as remarked by Kock [3], the inclusions effectively react to radio waves in a manner not unlike molecules of matter reacting to optical waves in the classical sense. An electric (or magnetic) field present in the artificial material induces a charge separation and current on each inclusion, giving rise to microscopic electric and magnetic multipole moments; when the equations are averaged in the usual sense, an electric polarization and magnetization may be defined that are analogous to the electric polarization and magnetization associated with real matter. These macroscopic polarizations are a result of the microscopic structure of the artificial material and lead to modifications of the effective permittivity and permeability of the (macroscopic) medium.

Design of an artificial material includes determining the density, arrangement, composition, and structure of the inclusions; as pointed out by Blanchard *et al.* [4], an interesting feature of such freedoms is the potential of engineering a material exhibiting desired permittivity, permeability, and dispersion characteristics. By properly designing the inclusions, many natural optical effects can be synthesized at suboptical (usually microwave) frequencies; effects such as anisotropy (e.g., [5]), temporal dispersion (e.g., [6]), chirality (e.g., [7]), and inhomogeneity (e.g., see the review article by Brown [8, pp. 221–222] and works referenced therein) have already been investigated. To produce these effects, the inclusions in artificial material are often developed with a certain microscopic optical model in mind. For example, anisotropy in real dielectrics may occur whenever the molecules comprising the dielectric are asymmetric (assuming the molecules have the same orientation throughout the dielectric); the molecular asymmetry results in microscopic charge and current distributions that depend upon the orientation of the polarizing electric and magnetic fields. In a similar fashion, the inclusions that give rise to anisotropy in artificial materials are those not possessing spherical symmetry, two examples being the long wire [5] and the strip [2, p. 774]. As another example, certain molecules may have no center of symmetry so media comprised of such molecules display natural optical activity (rotation of the polarization plane of linearly polarized light); the counterpart inclusions in artificial materials are chiral objects

such as the stemmed one-turn helix described by Jaggard *et al.* [7]. In recent years, studies of chiral media and, in general, bianisotropic media have gained considerable interest, particularly in regard to synthetically creating such media by means of artificial materials. To accurately predict wave behavior in artificial chiral media, a number of researchers have developed sophisticated models for chiral inclusions (e.g., [6], [7], [9]–[15]).

Continuing along this line of thought, one effect that appears to have received less attention by designers of artificial material is the idea of *macroscopic* spatial *feedback*, whereby electromagnetic fields in one region of space can *influence* the microscopic charge and current distributions (and, when averaged properly, the *macroscopic* induced polarizations) in another region of space. The phenomenon of microscopic spatial nonlocality is not new; as is well known in the field of crystal optics, certain crystals, when excited near an exciton resonance band, may exhibit microscopic nonlocal effects [16], [17, ch. 5]. Our interests here are to explore how *macroscopic* nonlocality might be engineered into an artificial material and to understand what effects *macroscopic* nonlocality might have on wave propagation.

Researchers have demonstrated that microscopic nonlocality introduces spatial dispersion (e.g., [18]), so we anticipate similar findings for macroscopic nonlocality in artificial material. Spatial dispersion refers to the feature of a material to exhibit certain properties that depend upon the magnitude and/or direction of the vector wavenumber. As mentioned by Felsen and Marcuvitz [19, p. 75], spatially dispersive media can be described in the space–time domain by reduced[1] constitutive relations that have direct dependence on at least one spatial derivative. In principle, an infinite number of these spatial derivatives would be required to write point-wise constitutive relations for nonlocal media; as an alternative, the constitutive relations themselves may be written as nonlocal relations.

II. THE IDEA OF ARTIFICIAL FEEDFORWARD–FEEDBACKWARD MEDIA

How might macroscopic nonlocality be introduced into an artificial material? In effect, we require inclusions constructed in such a manner that their dipole moments may be influenced not only by the electromagnetic fields interacting with any given inclusion, but also by the electromagnetic fields interacting with at least one other inclusion some *macroscopic* distance away. Conceptually, one might theoretically accomplish this, as suggested by Saadoun and Engheta [20], [21], by joining pairs of inclusions with *tiny transmission lines*. Issues regarding the direct interaction of the electromagnetic fields with these tiny transmission lines themselves must be accounted for, but otherwise one can model the material as producing polarization and/or magnetization at one location partly[2] in response to fields at another location—exactly what
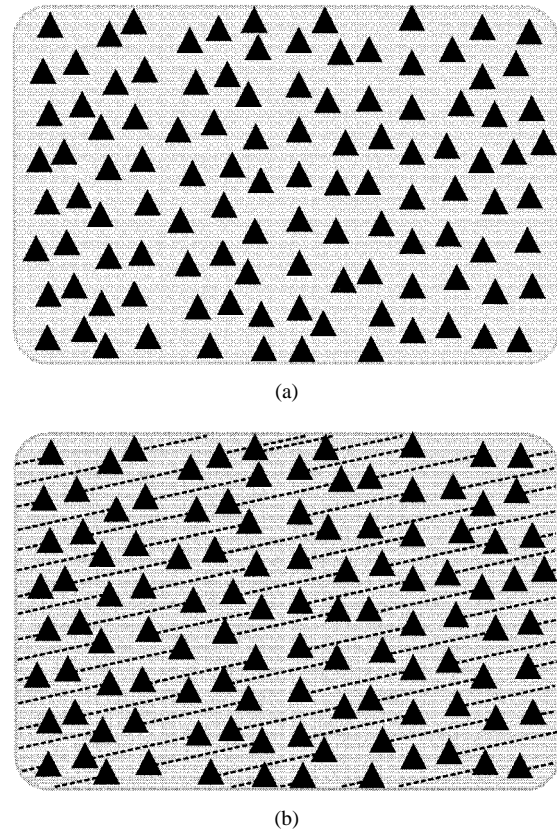

(a)

(b)

Fig. 1. The conceptualization of an artificial FFFB medium. (a) A local artificial material. The pyramids represent generic inclusions embedded within the host medium. (b) By joining pairs of inclusions, one conceptually creates the FFFB medium; the end-inclusions may be linked by parallel tiny two-wire transmission lines (shown as single dotted lines).

is desired of macroscopic nonlocal media. As causality requires, the nonlocal polarization and magnetization responses are not instantaneous due to the finite speed of wave propagation along a (tiny) transmission line.

The arrangement we are imagining can be conceptually constructed as follows [22]. First one would take a random distribution of electrically small conducting objects dispersed throughout some host medium [as in conventional artificial material; see Fig. 1(a)], then, by means of many parallel tiny transmission lines, one would conceptually link every inclusion in the medium to one other inclusion some fixed distance away [Fig. 1(b)]. The connection between the transmission line and an end inclusion can be made by physically splitting the end inclusion into two separate parts and then by connecting each of the two wires of one tiny transmission line to a different part. We label artificial material conceptually prepared by linking many pairs of inclusions in this manner as artificial "feedforward–feedbackward" (FFFB) media; the adjective *feedforward–feedbackward* is meant to convey the notion that the medium samples the field at every *macroscopic*[3] *point* and carries the effect of that sample both forward and

---

[1] The word *reduced*, as mentioned by Felsen and Marcuvitz, is used to indicate that all the properties of the medium (both electromagnetic and nonelectromagnetic) are lumped into permittivity and permeability dyadics [19, sec. 1.5].

[2] We say partly because the end-inclusion itself necessarily gives rise to polarization and/or magnetization fields as in conventional artificial material.

[3] As with conventional dielectrics, we are (usually) not interested in the field surrounding the inclusions; instead, we are primarily interested in the average field, averaged over a (macroscopically small) volume containing a large number of small inclusions. In this sense, a *macroscopic point* refers to a point within a (macroscopically small) volume δV that contains a large number of small inclusions.

backward (in space) to induce polarization and/or magneti-
zation at some displaced *point*, analogous to the feedback
concept of lumped (or distributed) circuits. Saadoun and
Engheta [21] theoretically investigated a nonlocal artificial
material (the nonlocal Ω medium) composed of inclusions
conceptually formed by linking a short dipole to a small
conducting loop through a length of tiny transmission line.
Located randomly, but each with the same orientation, these
coupled inclusions were shown to lead to macroscopic non-
local properties by inducing an electric (magnetic) dipole
moment at one location partly in response to a magnetic
(electric) field displaced some fixed relative distance. The
length and other properties of the tiny transmission lines
introduce additional degrees of freedom that are not present
in local Ω media; these parameters might find some use in
designing artificial Ω material for certain applications.

As a generalization of nonlocal Ω media, we are interested
in examining the properties of a broader class of nonlocal
artificial material in which the end inclusions may take other
shapes. Here we consider the class of paired inclusions that
produce electric polarization at one point partly in response
to an electric field at some other point. More specifically,
we are interested in the case where both end inclusions are
short dipoles (*dipole–dipole media*); as shown in Fig. 2, paired
inclusions are located randomly within the supporting medium
but each pair has some fixed orientation. A discussion limited
to paired dipoles, although restrictive, still has a number of
degrees of freedom (see Fig. 3): we can specify the absolute
orientation and length of both end dipoles, the structure and
length of the tiny transmission line, and the length separating a
pair of end dipoles (the separation may be no greater than the
length of the transmission line). Dipole–dipole FFFB media
may be theoretically investigated by accounting for the effects
of the paired inclusions through nonlocal constitutive relations
and then by solving the macroscopic Maxwell equations.
As shown in this paper, the constitutive relations can be
determined by making circuit model (quasi-static) approxima-
tions for the polarizability of each end-inclusion, but applying
transmission line theory for the tiny transmission line and
then by averaging the total polarizability over a large number
of inclusions to find the medium polarization. As such, we
require the end dipoles themselves to be thin and electrically
small; however, we do not require the two end dipoles of each
paired-dipole inclusion to necessarily have close proximity
because their finite separation will be taken into account
through an analysis of the transmission line when we deduce
the dipole–dipole FFFB media constitutive relations.

III. CALCULATION OF DIPOLE–DIPOLE FFFB MEDIUM PARAMETERS

Study of the electromagnetic properties of any (artificial)
material requires one to first formulate a consistent elec-
tromagnetic model for that material and, in particular, for
its inclusions. By doing so we determine the appropriate
constitutive relations to be used with the Maxwell equations;
toward this end we begin our analysis by first considering the
dipole moments induced on each paired-dipole inclusion of the
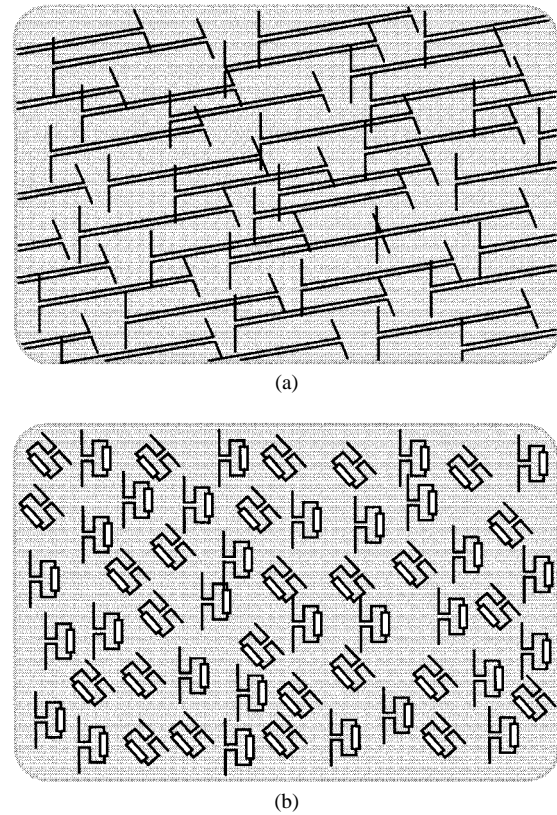

(a)

(b)

Fig. 2. One conceptualization of the dipole–dipole FFFB medium. (a) Here,
short dipoles are connected by a tiny two-wire transmission line. Although
the end dipoles need not be perpendicular to the transmission line as depicted
here and may, in general, have any orientation; we do require that every dipole
pair maintain some fixed orientation throughout the material. (b) The same
medium as in (a), however, each end dipole is connected to an equivalent
lumped element that represents the tiny transmission line and the other end
dipole. This lumped element depends upon the electric field present at the
location of the other end dipole as well as upon the characteristics of both the
transmission line and the other end dipole itself. In our analysis, the lumped
element includes a transmission line, an electromotive force, and a series
impedance.
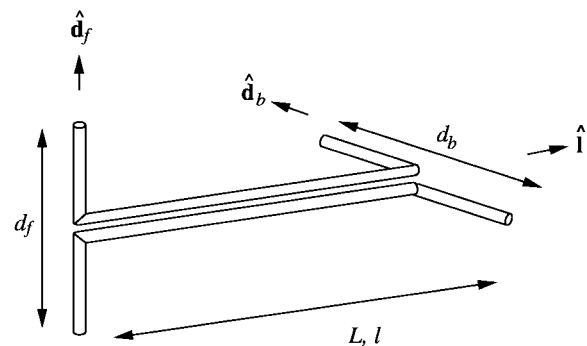
Fig. 3. Parameters of the paired dipole–dipole inclusions (used in
dipole–dipole FFFB media) include the absolute orientation of each dipole $\hat{\mathbf{d}}_f$
and $\hat{\mathbf{d}}_b$, the length of each dipole d_f, and d_b, the length of the transmission
line L, and the displacement of the dipoles $\mathbf{l} = l\hat{\mathbf{l}}$. In this figure, the dipole
separation l and transmission line length L are equal.

dipole–dipole FFFB medium. For a single arbitrarily oriented
short dipole, the parallel time-harmonic electric field develops
a time-harmonic charge displacement and concomitant current
on each dipole stem; as a consequence, a single electric dipole
moment is induced. In the same manner, but for the paired-

dipole inclusion (shown in Fig. 3), a total of four dipole moments are induced[4]:

$$
\begin{aligned}
\boldsymbol{p}_{ff}(\boldsymbol{r}) &= \epsilon_o \alpha_{ff} [\hat{\boldsymbol{d}}_f \cdot \boldsymbol{E}(\boldsymbol{r})] \hat{\boldsymbol{d}}_f \\
\boldsymbol{p}_{bf}(\boldsymbol{r}) &= \epsilon_o \alpha_{bf} [\hat{\boldsymbol{d}}_f \cdot \boldsymbol{E}(\boldsymbol{r} - \boldsymbol{l})] \hat{\boldsymbol{d}}_b \\
\boldsymbol{p}_{bb}(\boldsymbol{r}) &= \epsilon_o \alpha_{bb} [\hat{\boldsymbol{d}}_b \cdot \boldsymbol{E}(\boldsymbol{r})] \hat{\boldsymbol{d}}_b \\
\boldsymbol{p}_{fb}(\boldsymbol{r}) &= \epsilon_o \alpha_{fb} [\hat{\boldsymbol{d}}_b \cdot \boldsymbol{E}(\boldsymbol{r} + \boldsymbol{l})] \hat{\boldsymbol{d}}_f.
\end{aligned} \tag{1}
$$

Here, α_{ij} are the polarizabilities, $\boldsymbol{l}$ is the displacement from the front dipole to the back dipole, and $\hat{\boldsymbol{d}}_j$ are unit vectors indicating the orientation of the end dipoles as shown in Fig. 3. The subscripts f and b refer to the front and back dipoles, respectively; therefore, the moment $\boldsymbol{p}_{bf}(\boldsymbol{r})$ is the dipole moment produced by charge displacement on the *back* dipole due to an electric field across the *front* dipole. The tiny transmission line is assumed to connect the stems with the sense shown; reversing this connection (i.e., putting a single twist in the tiny transmission line) is tantamount to flipping the sign of either $\hat{\boldsymbol{d}}_b$ or $\hat{\boldsymbol{d}}_f$ (but not both).

The electromagnetic fields may also interact *directly* with the tiny transmission lines. An electric field component parallel to the tiny transmission line will induce currents directly on both wires of the tiny transmission line; these currents may depend upon the direction of propagation as well as upon the orientation of the electric field vector. The effects of these currents on wave propagation may be somewhat similar to those appearing in unidirectionally conducting screens [23] or superdense dipole arrays [24]. For axial plane wave propagation (i.e., propagation along the axis of the transmission line) and for end dipoles oriented perpendicularly to the transmission line, the wave has no electric or magnetic field components along the direction of propagation (the wave is TEM) and, therefore, the aforementioned transmission line currents are not generated. In this paper, we only study the case of propagation of plane waves in the axial direction, so by virtue of this restriction, the direct interaction of electromagnetic fields with the transmission lines is not taken into account.

A. Circuit Model Analysis

To calculate the induced dipole moments (1), we first determine the approximate current and charge distributions along the end dipoles when they are illuminated by a plane wave, and then find the moments of these charge distributions. For example, consider a short center-loaded dipole with length d and radius a (with $a \ll d$) connected to a load impedance Z_L. One well-known expression for the current along such a dipole[5] is given by King [25, pp. 464–467] as

$$
I(z) \doteq \frac{E_o \cos \psi}{k_o \sin \theta} \left[u_o(z) - v_o(z) \frac{Z_A Z_L}{Z_A + Z_L} u_o(0) \right]
$$
$$
\text{from King} \quad [25, \text{IV. } 4.15] \tag{2}
$$

for plane wave illumination where (with $e^{j\omega t}$ time dependence

---

[4] MKS units are used throughout; accordingly, $\mu_o = 4\pi \cdot 10^{-7}$ H/m and $\epsilon_o \doteq 8.854 \cdot 10^{-12}$ F/m.

[5] Without lack of generality, the dipole is taken to coincide with the z axis, extending from $z = -d/2$ to $z = +d/2$.

suppressed)

$$
u_o(z) = \frac{j4\pi}{\eta_o \Psi} \left(\frac{\cos(k_o z) \cos[\frac{1}{2} k_o d \cos(\theta)] - \cos(k_o z \cos \theta) \cos(\frac{1}{2} k_o d)}{\cos(\frac{1}{2} k_o d)} \right)
$$
$$
\text{from King} \quad [25, \text{Eqn. IV. } 3.26] \tag{3}
$$

$$
v_o(z) = \frac{j2\pi}{\eta_o \Psi} \frac{\sin[\frac{1}{2} k_o (d - 2|z|)]}{\cos(\frac{1}{2} k_o d)}
$$
$$
\text{from King} \quad [25, \text{Eqn. IV. } 3.27]. \tag{4}
$$

In (2), the term involving $u_o(z)$ is an approximate expression for the current induced on a thin conducting cylinder, the term involving $v_o(z)$ is an approximate expression for the current impressed on a dipole antenna due to a voltage source at its terminals, and $\Psi \doteq \Omega - 2 - 2\ln 2$ (with $\Omega = 2\ln d/a$) is a parameter referred to by King [25, p. 184] as the expansion parameter (for short dipoles), which relates the wire current to the magnitude of the vector potential just outside the wire surface. The impedances Z_A, Z_L, and η_o are, respectively, the input impedance of the dipole (viewed in transmitting mode), the load impedance connected at the dipole terminals, and the intrinsic impedance of the host medium. The wavenumber k_o corresponds to the wavenumber in the host medium, the angle θ is the angle between the wavevector of the illuminating plane wave and the dipole axis and ψ is the angle between the electric field vector and the plane containing both the wavevector and the dipole axis. By E_o, we denote the magnitude of the incident electric field transverse to the direction of propagation of the incident wave. By invoking the equation of continuity $q(z) = -(1/j\omega)dI(z)/dz$, one can determine the corresponding charge distribution along the antenna. Then, by taking the first moment of the charge distribution and neglecting higher order terms of $k_o d$, one finds the following expression for the dipole moment of a short dipole:

$$
\boldsymbol{p} = \left(\frac{E_o d^2 \cos \psi \sin \theta}{12 j\omega Z_A} + \frac{E_o d^2 \cos \psi \sin \theta}{4 j\omega (Z_A + Z_L)} \right) \hat{z}. \tag{5}
$$

The first term approximates the dipole moment due to the two stems of the dipole when the load is replaced by an open circuit; for reference, we denote this contribution by $\boldsymbol{p}^{\text{stems}}$. The second term incorporates the effects of the load and can be shown to have a circuit analog when the quasi-static approach is employed. In this approach (e.g., [6], [21]), the electric field induces a quasi-static electromotive force across the dipole terminals $\mathcal{E}_A = E_o d_e \cos \psi \sin \theta$ bringing about a current I at the dipole terminals $I = \mathcal{E}_A/(Z_A + Z_L)$. The input impedance Z_A of a cylindrical dipole having some particular length and radius may be read from a chart (e.g., [25, p. 155], [26, sec. 4-2]) or may be calculated by various analytical and numerical techniques (e.g., [25, sec. II.27], [27], [28, ch. 7]). For our purposes, we use the approximate analytical expression from King [25, p. 192] for the reactive component of the impedance of a short dipole

$$
X_A \doteq \frac{-120(\Omega - 2 - 2\ln 2)}{k_o d} \quad \text{(Ohms)}
$$
$$
\text{from King} \quad [25, \text{Eqn. II. } 31.50] \tag{6}
$$

and rewrite here King's approximate expression [25, p. 192] for the input resistance of a short dipole for $\Omega = 10$

$$R_A \doteq 4.58(k_o d)^2 [1 + 0.022(k_o d)^2] \text{ (Ohms)}$$
$$\text{from King} \quad [25, \text{Eqn. II. } 31.46\text{a}]. \quad (7)$$

The input impedance is clearly largely reactive for very short dipoles and, thus, we only take the reactive part of the input impedance into account in our model and neglect the resistive part. The effective length[6] d_e appearing in the equation for $\mathcal{E}$ is given by $d_e \doteq d/2$ for short thin dipoles.

The time-harmonic dipole moment $\boldsymbol{p}$ is determined by the charge and its displacement, $\boldsymbol{p} = Q d_e \hat{\boldsymbol{d}}$, with $\hat{\boldsymbol{d}}$ a unit vector indicating the direction of the dipole moment, d_e the antenna effective length, and Q the displaced positive charge. Noting $I = j\omega Q$, the dipole moment reads: $\boldsymbol{p} = [d^2 E_o \cos\psi \sin\theta]/[4j\omega(Z_A + Z_L)]\hat{\boldsymbol{d}}$ as before [compare this expression to the second term in (5)]. Therefore, if we know the current I at the dipole terminals, we can follow the above quasi-static technique to find one portion of the induced dipole moment. To determine the appropriate form of this dipole moment for the inclusions of dipole–dipole FFFB media, we use a Thevenin equivalent circuit [29, p. 68], [30, p. 43] for each end dipole and then use transmission line theory to determine the terminal currents of the paired end dipoles. To this dipole moment we then add the first term of (5) corresponding to the dipole moment arising from polarization of the individual stems of the end dipoles ($\boldsymbol{p}^{\text{stems}}$).

B. Transmission-Line Analysis

Analysis of the transmission line circuit shows that the terminal currents are given by

$$I_f = \frac{-\mathcal{E}_b + \mathcal{E}_f \left(\cosh\gamma L + \dfrac{Z_f}{Z_o}\sinh\gamma L \right)}{(Z_f + Z_b)\cosh\gamma L + \left(Z_o + \dfrac{Z_f Z_b}{Z_o} \right)\sinh\gamma L}$$

$$I_b = \frac{-\mathcal{E}_f + \mathcal{E}_b \left(\cosh\gamma L + \dfrac{Z_b}{Z_o}\sinh\gamma L \right)}{(Z_f + Z_b)\cosh\gamma L + \left(Z_o + \dfrac{Z_f Z_b}{Z_o} \right)\sinh\gamma L} \quad (8)$$

where the subscripts f and b refer to the *front* and the *back* dipole inclusions; accordingly, Z_f and Z_b represent the input impedances of the front and back dipoles, respectively, and I_f and I_b represent the current flowing into the front and back dipole terminals, respectively, from the transmission line. The transmission line of length[7] L is described by a complex

---

[6] The effective antenna length referred to here coincides with the definition supplied by King [29, p. 68]: $d_e = I Z_A / E_{\text{inc}}$, where I is the terminal current of a symmetric unloaded dipole antenna, Z_A is the antenna input impedance (when the corresponding antenna is used in transmit mode), and E_{inc} is the magnitude of the parallel normally incident plane wave electric field. Physically, this definition corresponds to the voltage induced across the open-circuit terminals of a dipole, divided by the electric field magnitude exciting the dipole.

[7] In general, the transmission line length L and the dipole separation l can be independent variables, related only by the constraint $l \leq L$. However, in this paper, we always take $l = L$. Here L should not be mistaken for the customary variable representing inductance.

propagation constant γ and a characteristic impedance Z_o. In our approximations, the transmission-line wavenumber is not influenced by the polarizability of the medium; the characteristic impedance depends upon the geometry of the transmission line, which we take to be a two-wire transmission line having closely spaced thin conductors of circular cross section.

Now we follow the previously demonstrated procedure to determine all four polarizabilities $\alpha_{ff}, \alpha_{bb}, \alpha_{fb}$, and α_{bf} as defined in (1); to determine α_{ff}, set $\mathcal{E}_b = 0$, $\mathcal{E}_f = E_o(\boldsymbol{r})d_f/2$, and use I_f as the polarizing current in the expression for the dipole moment

$$\boldsymbol{p}_{ff}(\boldsymbol{r}) = \epsilon_o \alpha_{ff} \hat{\boldsymbol{d}}_f [\hat{\boldsymbol{d}}_f \cdot \boldsymbol{E}(\boldsymbol{r})] = \frac{I_f d_f \hat{\boldsymbol{d}}_f}{2j\omega} + \boldsymbol{p}^{\text{stems}}. \quad (9)$$

Solving for α_{ff} yields

$$\alpha_{ff} = \frac{d_f^2}{12jk_o} \left[\frac{\eta_o}{Z_f} + \frac{3\eta_o}{Z_f + \text{TL}(Z_b)} \right] \quad (10)$$

where $\text{TL}(Z) = Z_o[Z\cosh(\gamma L) + Z_o\sinh(\gamma L)]/[Z_o\cosh(\gamma L) + Z\sinh(\gamma L)]$ is the apparent impedance of a load Z as seen through a length L of transmission line with parameters γ and Z_o. A similar procedure establishes the back–back polarizability

$$\alpha_{bb} = \frac{d_b^2}{12jk_o} \left[\frac{\eta_o}{Z_b} + \frac{3\eta_o}{Z_b + \text{TL}(Z_f)} \right]. \quad (11)$$

For the front–back and back–front polarizabilities, we use electromotive forces and currents at opposite ends of the transmission line; as an example, for α_{fb} set $\mathcal{E}_f = 0, \mathcal{E}_b = E_o(\boldsymbol{r} + \boldsymbol{l})d_b/2$ and use I_f as the polarizing current

$$\boldsymbol{p}_{fb}(\boldsymbol{r}) = \epsilon_o \alpha_{fb} \hat{\boldsymbol{d}}_f [\hat{\boldsymbol{d}}_b \cdot \boldsymbol{E}(\boldsymbol{r} + \boldsymbol{l})] = \frac{I_f d_f \hat{\boldsymbol{d}}_f}{2j\omega} \quad (12)$$

yielding the front-back polarizability

$$\alpha_{fb} = \frac{d_b d_f}{4jk_o}$$
$$\cdot \left[\frac{-\eta_o}{(Z_f + Z_b)\cosh\gamma L + \left(Z_o + \dfrac{Z_f Z_b}{Z_o} \right)\sinh\gamma L} \right]. \quad (13)$$

As our circuit model predicts (and as a necessary condition for reciprocity), the back–front polarizability has an identical expression, so $\alpha_{bf} = \alpha_{fb}$.

C. Illustrative Examples

Before we proceed to use these polarizabilities in analyzing bulk FFFB media, we examine the dipole moments and polarizabilities as expressed in (1), (10), (11), and (13) for some special cases. The first case we consider is the limit when the end dipoles are directly connected together (i.e., $l = L = 0$) and are identical ($d \equiv d_b = d_f$; correspondingly,

$Z \equiv Z_b = Z_f$ is the input impedance of either end dipole). For these parameters, the above dipole moments reduce to

$$\boldsymbol{p}_{ff}(\boldsymbol{r}) = \frac{5d^2}{24j\omega Z}\hat{\boldsymbol{d}}_f\hat{\boldsymbol{d}}_f \cdot \boldsymbol{E}(\boldsymbol{r}), \quad \boldsymbol{p}_{bb}(\boldsymbol{r}) = \frac{5d^2}{24j\omega Z}\hat{\boldsymbol{d}}_b\hat{\boldsymbol{d}}_b \cdot \boldsymbol{E}(\boldsymbol{r})$$

$$\boldsymbol{p}_{fb}(\boldsymbol{r}) = \frac{-d^2}{8j\omega Z}\hat{\boldsymbol{d}}_f\hat{\boldsymbol{d}}_b \cdot \boldsymbol{E}(\boldsymbol{r}), \quad \boldsymbol{p}_{bf}(\boldsymbol{r}) = \frac{-d^2}{8j\omega Z}\hat{\boldsymbol{d}}_b\hat{\boldsymbol{d}}_f \cdot \boldsymbol{E}(\boldsymbol{r}).$$

$$(14)$$

To construct an artificial material with these inclusions, one would conceptually position dipole pairs at random locations throughout the host medium (although all inclusions would have some fixed orientation); we denote by n the number of front-dipoles per unit volume.[8] If n is not too large and if we neglect interaction among neighboring inclusions,[9] then the net polarization at any macroscopic point is given by the sum $\boldsymbol{P}(\boldsymbol{r}) = n\boldsymbol{p}(\boldsymbol{r}) = n[\boldsymbol{p}_{ff}(\boldsymbol{r}) + \boldsymbol{p}_{bb}(\boldsymbol{r}) + \boldsymbol{p}_{bf}(\boldsymbol{r}) + \boldsymbol{p}_{fb}(\boldsymbol{r})]$. When $\hat{\boldsymbol{d}}_b$ and $\hat{\boldsymbol{d}}_f$ are collinear, then either $\boldsymbol{p}(\boldsymbol{r}) = 2\boldsymbol{p}^{\mathrm{stems}}$ or $\boldsymbol{p}(\boldsymbol{r}) = 8\boldsymbol{p}^{\mathrm{stems}}$ depending on whether $\hat{\boldsymbol{d}}_b = \hat{\boldsymbol{d}}_f$ or $\hat{\boldsymbol{d}}_b = -\hat{\boldsymbol{d}}_f$, respectively (as shown in Fig. 4(a) and (b)]. Now suppose $\hat{\boldsymbol{d}}_f$ and $\hat{\boldsymbol{d}}_b$ are not collinear; then the transverse electric field[10] has two components that can be expressed in a $(\hat{\boldsymbol{d}}_b + \hat{\boldsymbol{d}}_f, \hat{\boldsymbol{d}}_f - \hat{\boldsymbol{d}}_b)$ basis

$$\boldsymbol{E}(\boldsymbol{r}) = E_+(\boldsymbol{r})\left(\frac{\hat{\boldsymbol{d}}_f + \hat{\boldsymbol{d}}_b}{|\hat{\boldsymbol{d}}_f + \hat{\boldsymbol{d}}_b|}\right) + E_-(\boldsymbol{r})\left(\frac{\hat{\boldsymbol{d}}_f - \hat{\boldsymbol{d}}_b}{|\hat{\boldsymbol{d}}_f - \hat{\boldsymbol{d}}_b|}\right). \quad (15)$$

In terms of these components of $\boldsymbol{E}(\boldsymbol{r})$, the total dipole moment reads

$$\boldsymbol{p}(\boldsymbol{r},\omega) = E_-(\boldsymbol{r})\frac{d^2}{3j\omega Z}[1 - (\hat{\boldsymbol{d}}_b \cdot \hat{\boldsymbol{d}}_f)]\left(\frac{\hat{\boldsymbol{d}}_f - \hat{\boldsymbol{d}}_b}{|\hat{\boldsymbol{d}}_f - \hat{\boldsymbol{d}}_b|}\right)$$
$$+ E_+(\boldsymbol{r})\frac{d^2}{12j\omega Z}[1 + (\hat{\boldsymbol{d}}_b \cdot \hat{\boldsymbol{d}}_f)]\left(\frac{\hat{\boldsymbol{d}}_f + \hat{\boldsymbol{d}}_b}{|\hat{\boldsymbol{d}}_f + \hat{\boldsymbol{d}}_b|}\right).$$

$$(16)$$

As can be seen from Fig. 4(c) and (d), E_+ only induces dipole moments across individual dipole stems since the current vanishes at the antenna terminals. On the other hand, E_- induces a dipole moment across the entire paired-dipole inclusion since the antenna terminal currents do not vanish.

As a numerical example, we investigate the polarizabilities for two particular sets of parameters. Specifically for the purpose of plotting, we choose the fixed value $d = 0.1\lambda_o$ with transmission line parameters $\gamma = jk_o = j2\pi/\lambda_o$ and $Z_o = 0.93\eta_o$ and plot the two unique polarizabilities $\alpha \equiv \alpha_{ff} = \alpha_{bb}$ and $\beta \equiv \alpha_{bf} = \alpha_{fb}$ from (11) and (13) as a function of normalized transmission line length $\Delta = L/\lambda_o$ for dipoles of two different radii ($\Omega = 6$ and $\Omega = 10$). These plots are shown in Fig. 5. Notice the sharp resonances that appear when L is just short of integer multiples of $\lambda_o/2$. In reality, such sharp resonances would be broadened because of dissipation

[8] Since all the end dipoles are paired, the density of back-dipoles is the same as that of front-dipoles; as a result, in total there are $2n$ dipole inclusions per unit volume distributed throughout the host medium.

[9] In the next section, we indicate Lorentz theory modifications that should be made to the medium polarization to account for quasi-static interaction among neighboring inclusions.

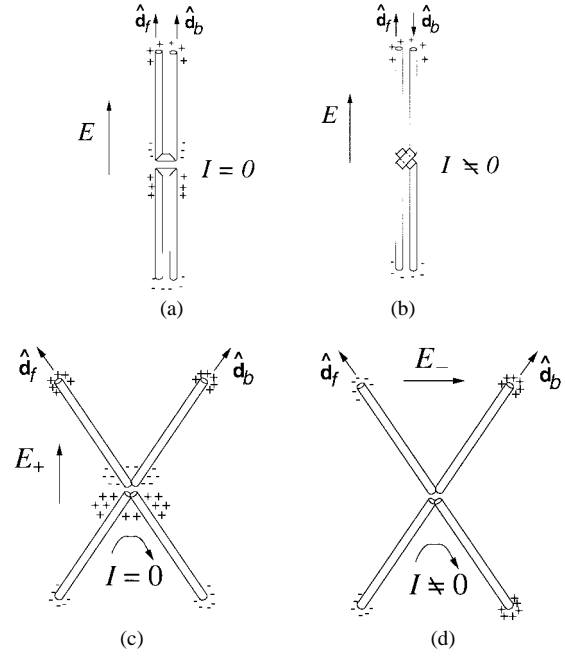[10] Transverse in the plane formed by $\hat{\boldsymbol{d}}_b$ and $\hat{\boldsymbol{d}}_f$.

Fig. 4. Polarization of the dipole–dipole inclusions in the limit $L = 0$ for collinear $\hat{\boldsymbol{d}}_b$ and $\hat{\boldsymbol{d}}_f$. (a) The only polarization arises from the polarization of the individual dipole stems since I vanishes at the terminals. However, here in (b), the current at the terminals does not vanish and dipole moments are induced across the entire dipole. Polarization of the dipole–dipole inclusions in the limit $L = 0$ for noncollinear $\hat{\boldsymbol{d}}_f$ and $\hat{\boldsymbol{d}}_b$. (c) There is again only polarization from the individual dipole stems since the current I vanishes at the terminals. However, here in (d), the current at the terminals does not vanish so there are induced dipole moments across the entire paired-dipole inclusion.

in both the transmission line and its terminations, as well as tolerances in the lengths of the transmission lines. The nature of these resonances is similar to those observed in lumped L-C circuits; since both end dipoles have been replaced by reactive elements (capacitances), then for some length of transmission line the reactance of one end dipole will be transformed into the conjugate reactance (an inductance) of the other end dipole causing the entire circuit to resonate at the operating frequency. Since thin dipoles have a larger negative input reactance than do thick dipoles, the polarizabilities corresponding to $\Omega = 10$ do not have as much variation in the nonresonance regions as do those for $\Omega = 6$. Also, since the input reactances for $\Omega = 6$ and $\Omega = 10$ are different, we notice that slightly different lengths of transmission line are required to bring the circuit into resonance.

When the end dipoles and the connecting tiny transmission line are mutually perpendicular, then we name the inclusions *crossed-dipole feedforward–feedbackward* inclusions. If now these paired dipole inclusions are dispersed throughout a host medium, then we name the resulting media *crossed-dipole feedforward–feedbackward* media. The paired-dipole inclusions are placed at random locations within the host medium; however, the orientation of each inclusion is the same. Here, we choose the front dipole parallel to the x axis, the back dipole parallel to the y axis, and the transmission line along the z axis (i.e., $\hat{\boldsymbol{d}}_f = \hat{\boldsymbol{x}}$, $\hat{\boldsymbol{d}}_b = -\hat{\boldsymbol{y}}$, and $\boldsymbol{l} = l\hat{z}$). Notice that because of the connection of the stems through the tiny transmission line (see Fig. 3), $\hat{\boldsymbol{d}}_b$ is associated with $-\hat{\boldsymbol{y}}$ (rather than $\hat{\boldsymbol{y}}$).
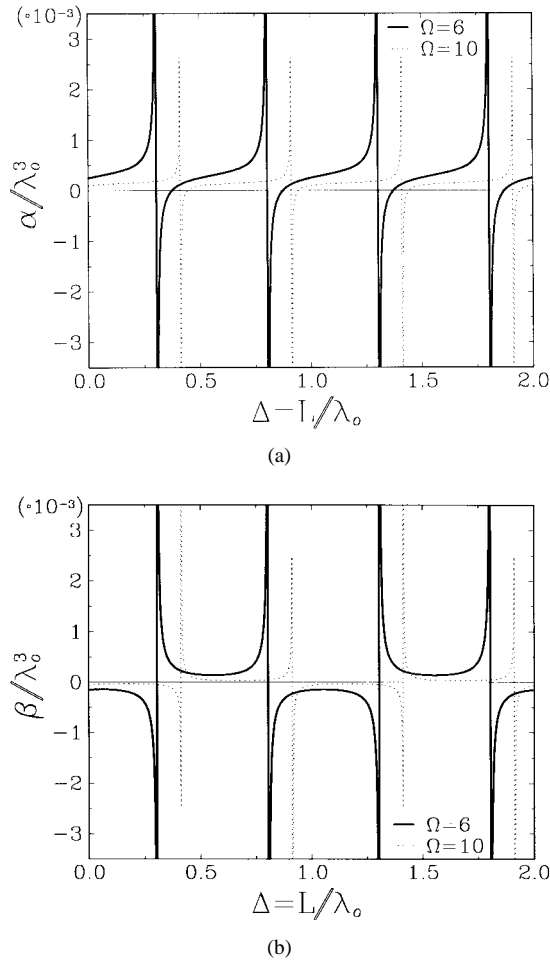
Fig. 5. (a) The normalized polarizability α/λ_o^3 as a function of normalized length $\Delta = L/\lambda_o$ for two dipoles of two different radii ($\Omega = 6$ and $\Omega = 10$). (b) The normalized polarizability β/λ_o^3 as a function of normalized length $\Delta = L/\lambda_o$. In both figures, for the purpose of plotting we set $d = 0.1 \lambda_o$, $\gamma = jk_o$, $Z_o = 0.93 \eta_o$, and *fix the frequency of operation*, allowing the length of the tiny transmission line (L) to vary.

D. Lorentz Theory Applied to Feedforward–Feedbackward Media

When the dimensions and density of the polarizable inclusions comprising the material are such that interaction between neighboring elements is primarily through the electric dipole term alone, then Lorentz theory (e.g., [31, sec. 4.5], [2, sec. 12.1]) can be used to determine the effective polarizability of the bulk medium. As a consequence, the influence of the inclusions can be described by a net electric dipole moment per unit volume $P_d(r)$.

Although the Lorentz theory requires the inclusions themselves to be small, the use of Lorentz theory for FFFB media does not require the overall paired dipole structure to be small since the role of the connecting length of tiny transmission line is handled through the nonlocal constitutive relations (shown shortly). Referring again to Fig. 2(b), each end dipole can be modeled as an element (with field-dependent characteristics) connected to the opposite dipole through a length of tiny transmission line. In this way, the medium *effectively* has loaded inclusions and can be similar to conventional artificial material. (Of course the nonlocal field dependent nature of

the element is entirely different from conventional inclusion loads.) At the same time, when the averaging process is carried out, we only average over a volume whose dimensions are large compared to one end inclusion and not necessarily large compared to the entire paired dipole structure (otherwise, the macroscopic nonlocal effects would vanish in the averaging). Other than these slight modifications, the Lorentz theory as applied to local artificial material is directly applicable to nonlocal artificial material. This being the case, we recall that the Lorentz field (viz., the polarizing, or effective field) is given by $E_L(r) = E(r) + (1/3\epsilon_o)\langle P_d(r)\rangle$, where $E(r)$ is the average field (viz., the macroscopic field) and $\langle P_d(r)\rangle$ is the average dipole polarization in the medium, given by $\langle P_d(r)\rangle = np(r)$. Here, n is number of front inclusions (see footnote 8) per unit volume and $p(r)$ is the total dipole moment of any single pair of dipoles; specifically, $p(r) = p_{ff}(r) + p_{bb}(r) + p_{bf}(r) + p_{fb}(r)$. The brackets in $\langle P_d(r)\rangle$ serve as a reminder that the medium polarization is averaged over a microscopically large yet macroscopically small region of space; for sake of convenience and brevity, we hereafter drop the averaging notation and assume all field quantities are averaged over the same region of space.

Because $P_d(r)$ includes contributions from dislocated electric fields [see (1)], we move into the wave-vector domain by taking a spatial Fourier transform. Accordingly, the material equations in the k domain can be written as[11]

$$\tilde{P}(k) = \epsilon_o n \tilde{\bar{\bar{\alpha}}}(k) \cdot \tilde{E}_L(k) \tag{17a}$$

$$\tilde{D}(k) = \epsilon_o \tilde{E}(k) + \tilde{P}(k) \tag{17b}$$

$$\tilde{E}_L(k) = \tilde{E}(k) + \frac{1}{3\epsilon_o}\tilde{P}(k) \tag{17c}$$

$$\tilde{D}(k) = \epsilon_o \tilde{\bar{\bar{\epsilon}}}(k) \cdot \tilde{E}(k) \tag{17d}$$

where the tilde embellishment denotes a spatial Fourier transformed quantity. Here we associate $\tilde{P}_d(k)$ directly with the medium polarization $\tilde{P}(k)$, attributing all the medium polarization to the collection of dipole moments arising from the end dipoles. The quantity $\tilde{\bar{\bar{\alpha}}}(k)$ is determined by setting E_L as the polarizing field E in (1) and using the equation for $\langle P_d(r)\rangle$ to write an equation in the form (17a)

$$\tilde{\bar{\bar{\alpha}}}(k_z\hat{z}) = (\alpha_{ff}\hat{d}_f\hat{d}_f + \alpha_{bb}\hat{d}_b\hat{d}_b + \alpha_{bf}\hat{d}_b\hat{d}_f e^{+jk_z l} + \alpha_{fb}\hat{d}_f\hat{d}_b e^{-jk_z l}). \tag{18}$$

We note that in this medium, $\alpha_{fb} = \alpha_{bf}$; furthermore, in the study reported in this paper, the medium only exhibits a FFFB mechanism along the axial direction (viz., the z direction), so $\tilde{\bar{\bar{\alpha}}}$ only depends upon the axial wavenumber k_z. The constitutive relations can now be determined by substituting (17c) into (17a) and writing $\tilde{P}(k)$ in terms of the average field $\tilde{E}(k)$. Using the resulting expression for $\tilde{P}(k)$ in (17b), one finds

$$\tilde{D}(k) = \epsilon_o\{\bar{\bar{I}} + [\bar{\bar{I}} - \tfrac{1}{3}n\tilde{\bar{\bar{\alpha}}}(k)]^{-1} \cdot n\tilde{\bar{\bar{\alpha}}}(k)\} \cdot \tilde{E}(k). \tag{19}$$

---

[11] The main thrust of this paper is in studying the electromagnetic effects of a FFFB mechanism in artificial material and not in singling out a particular mixing rule to be used in modeling composite media. As a consequence, we use here one well-known method for finding the average dipole polarization and effective permittivity.

From (17d), one recognizes the term in braces as the anisotropic effective relative permittivity $\tilde{\bar{\bar{\epsilon}}}(\boldsymbol{k})$; in our model we take the effective permeability to be a scalar equal to that of the host medium (μ_o). For the crossed-dipole inclusions, $\bar{\bar{\alpha}}(\boldsymbol{k})$ is given by $\bar{\bar{\alpha}}(k_z\hat{z}) = [\hat{x}\hat{x}\alpha_{ff} + \hat{y}\hat{y}\alpha_{bb} - \hat{y}\hat{x}\alpha_{bf}e^{+jk_zl} - \hat{x}\hat{y}\alpha_{bf}e^{-jk_zl}]$ yielding a relative permittivity, in tensor notation (x,y,z) given by

$$\tilde{\bar{\bar{\epsilon}}}(k_z\hat{z}) = \begin{bmatrix} \epsilon_{xx} & \zeta e^{-jk_zl} & 0 \\ \zeta e^{+jk_zl} & \epsilon_{yy} & 0 \\ 0 & 0 & 1 \end{bmatrix} \qquad (20)$$

where

$$\epsilon_{xx} = \frac{(1 - \frac{1}{3}n\alpha_{bb})(1 + \frac{2}{3}n\alpha_{ff}) + 2(\frac{1}{3}n\alpha_{bf})^2}{(1 - \frac{1}{3}n\alpha_{bb})(1 - \frac{1}{3}n\alpha_{ff}) - (\frac{1}{3}n\alpha_{bf})^2} \qquad (21a)$$

$$\epsilon_{yy} = \frac{(1 - \frac{1}{3}n\alpha_{ff})(1 + \frac{2}{3}n\alpha_{bb}) + 2(\frac{1}{3}n\alpha_{bf})^2}{(1 - \frac{1}{3}n\alpha_{bb})(1 - \frac{1}{3}n\alpha_{ff}) - (\frac{1}{3}n\alpha_{bf})^2} \qquad (21b)$$

$$\zeta = \frac{-n\alpha_{bf}}{(1 - \frac{1}{3}n\alpha_{bb})(1 - \frac{1}{3}n\alpha_{ff}) - (\frac{1}{3}n\alpha_{bf})^2}. \qquad (21c)$$

Notice that $\hat{z} \cdot \tilde{\bar{\bar{\epsilon}}}(k_z\hat{z}) \cdot \hat{z}$ is unity since, in the present study, we have neglected *direct* interaction of the axial electromagnetic field with the transmission line. In these equations, the polarizabilities α_{bb}, α_{ff}, and α_{bf} $(= \alpha_{fb})$ are those reported in Section III-B.

IV. AXIAL PLANE WAVE PROPAGATION IN UNBOUNDED SOURCE-FREE CROSSED-DIPOLE FFFB MEDIA

Having already written the constitutive relations in the $\boldsymbol{k}$ domain (as indicated in the last section), the resulting wave equation in the $\boldsymbol{k}$ domain is algebraic:

$$\boldsymbol{k} \times [\boldsymbol{k} \times \tilde{\boldsymbol{E}}(\boldsymbol{k})] + \omega^2\mu_o\epsilon_o\tilde{\bar{\bar{\epsilon}}}(\boldsymbol{k}) \cdot \tilde{\boldsymbol{E}}(\boldsymbol{k}) = 0. \qquad (22)$$

Since, in this study, we are concerned only with axial propagation, we set $\boldsymbol{k} = k_z\hat{z}$ and then normalize k_z by $k_o = \omega\sqrt{\mu_o\epsilon_o}$ (the host wavenumber), finding

$$[s^2(\bar{\bar{I}} - \hat{z}\hat{z}) - \tilde{\bar{\bar{\epsilon}}}(k_os\hat{z})] \cdot \tilde{\boldsymbol{E}}(k_os\hat{z}) = 0 \qquad (23)$$

where $s = k_z/k_o$. Written out component-wise, the above equation represents a system of algebraic equations; we look for nontrivial solutions by setting the determinant of the bracketed term in the above equation to zero

$$\det[s^2(\bar{\bar{I}} - \hat{z}\hat{z}) - \tilde{\bar{\bar{\epsilon}}}(k_os\hat{z})] = 0. \qquad (24)$$

Equation (24) is the sought *dispersion relation* and as such it establishes the relationship between wavenumber k_os and frequency ω that must be satisfied for axial plane wave propagation in unbounded source-free crossed-dipole FFFB media. Once the eigenvalues s^2 are determined, the polarization eigenstates are easily obtained by substituting the eigenvalues back into (23) and satisfying the resulting algebraic system.

For crossed-dipole FFFB media, we first substitute the relative permittivity (20) into (24) and then solve (24) for the two roots $s_{1,2}^2$ given by

$$s_{1,2}^2 = \frac{\epsilon_{xx} + \epsilon_{yy}}{2} \pm \frac{1}{2}\sqrt{(\epsilon_{xx} - \epsilon_{yy})^2 + 4\zeta^2}. \qquad (25)$$

We now consider the special case when the end dipoles are identical; once $\alpha \equiv \alpha_{ff} = \alpha_{bb}$ and $\beta \equiv \alpha_{bf}$ in (21), then $\epsilon_{xx} = \epsilon_{yy}$; consequently, the two families of roots to the dispersion equation are given by the expression $s_{1,2}^2 = \epsilon_{xx} \pm \zeta$ with the corresponding polarization eigenstates

$$\boldsymbol{E}_1(z) = E_1(\hat{y}e^{j2\pi s_1\Delta} + \hat{x})e^{-jk_os_1z}$$
$$\boldsymbol{E}_2(z) = E_2(-\hat{y}e^{j2\pi s_2\Delta} + \hat{x})e^{-jk_os_2z}. \qquad (26)$$

Here, $\Delta = l/\lambda_o$ is the normalized dipole displacement[12] (λ_o is the host medium wavelength) and the superscripts (1) and (2) denote the first and second eigenstates, respectively. Provided $\sin(2\pi s_1\Delta)\sin(2\pi s_2\Delta) > 0$, the two elliptically polarized eigenstates are seen to have opposite senses of rotation. If the medium constituents (viz., the dipoles and their connecting transmission lines) are lossless and, if we look only at propagating solutions, then s_1 and s_2 are real and the magnitude $|\tilde{E}_y/\tilde{E}_x|$ is always unity. Notice that when $n\alpha \ll 1$ and $n\beta \ll 1$ (for instance, when the concentration density is made sufficiently small), then the normalized wavenumbers are given approximately by $s_{1,2} \approx 1 + (n/2)(\alpha \pm \beta)$. The difference between normalized axial wavenumbers $s_1 - s_2 = n\beta$ does not vanish since β is nowhere identically zero.[13] It is interesting to note that propagating waves traveling in the axial direction of this medium share certain features with waves propagating in isotropic chiral media; for example, the eigenstates of both media consist of counter-rotating fields with different wavenumbers; however, in crossed-dipole FFFB media, these eigenstates are, in general, elliptically polarized whereas in chiral media they are circularly polarized. Upon re-examination of the geometry of the crossed-dipole inclusions (see Fig. 3), we notice that if each crossed-dipole paired inclusion is divided by shearing the connecting tiny transmission line along its axis between the two wires, then both halves of the original inclusion are themselves chiral objects (with the same handedness for each half). Individually, each of these chiral inclusions resembles the chiral hook enantiomorph studied by Theron and Cloete [11].[14] Unlike isotropic artificial chiral media, which would be synthesized by randomly distributing small chiral inclusions with random orientations, the inclusions in our conceptualization for crossed-dipole FFFB media all have some fixed orientation (and are not necessarily small). Because of these differences, the eigenstates for crossed-dipole FFFB media are not, in general, circularly polarized (as would be the case for isotropic chiral media).

Plots of the normalized wavenumber as a function of normalized length (for certain parameters indicated in the caption) appear in Fig. 6; some features of these plots are worth mentioning. First, for $L = 0$ (i.e., local media), the normalized wavenumber s_1 is influenced only by polarization of the individual dipole stems, whereas the normalized

---

[12] Since $L = l$, the variable Δ defined here is the same as that defined earlier when used to indicate normalized transmission line length.

[13] Of course, the function β (and for that matter α) both vanish if d vanishes.

[14] As introduced by Tilston *et al.* [32] and later mentioned by Roy and Shafai [33], a single layer (rather than a medium) of certain properly-designed coupled-dipole inclusions—resembling the dipole–dipole inclusions investigated here—may have interesting application in the design of polarization selective surfaces for circular polarization.
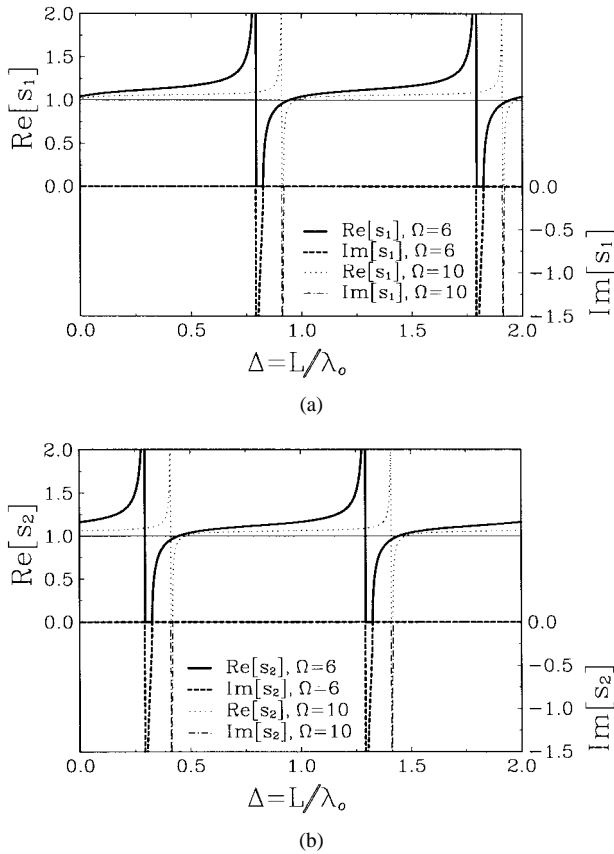
Fig. 6. Plots of normalized wavenumbers $(s = k_z/k_o)$ as functions of normalized transmission line length for two dipoles of different radii $(\Omega = 6$ and $\Omega = 10)$. (a) The first root to the dispersion equation. (b) The second root. In both figures, for the purpose of plotting, $n\lambda_o^3 = 800$, $d = 0.1\lambda_o$, $\gamma = jk_o$, $Z_o = 0.93\,\eta_o$, and we allow the transmission line length (L) to vary, *keeping the operating frequency fixed.*

wavenumber s_2 is larger since the corresponding wave induces dipole moments across the entire end dipole. For this case, observation of the corresponding polarization eigenstates shows that both wavenumbers are associated with linear polarized waves whose electric fields make an angle of either $-45°$ or $+45°$ to the positive x axis. As a result, one wave (s_2) strongly interacts with the dipole inclusions, while the other (s_1) does not interact as much. Next, we notice that for certain Δ the wavenumber experiences strong resonances and becomes completely imaginary[15] immediately following the resonances. In these regions, the wave is evanescent and, hence, carries no power. We notice that the evanescent regions occur for different Δ for the two different eigenstates. So while one wave may be evanescent, the other propagates freely; this feature might find some interesting potential application in the design of future microwaves devices utilizing such FFFB media. As seen by the differences between the plots for $\Omega = 6$ and $\Omega = 10$, it is possible to broaden the evanescent region by changing some parameters (especially the dipole input impedance). While our model may be inadequate to determine the exact field structure within these regions, one can speculate that evanescent regions will be present even if a more refined model is employed. Finally, we notice from Fig. 6 that, for

[15] As required by the condition of boundedness at infinity and because of our time convention, the imaginary part of s is negative.
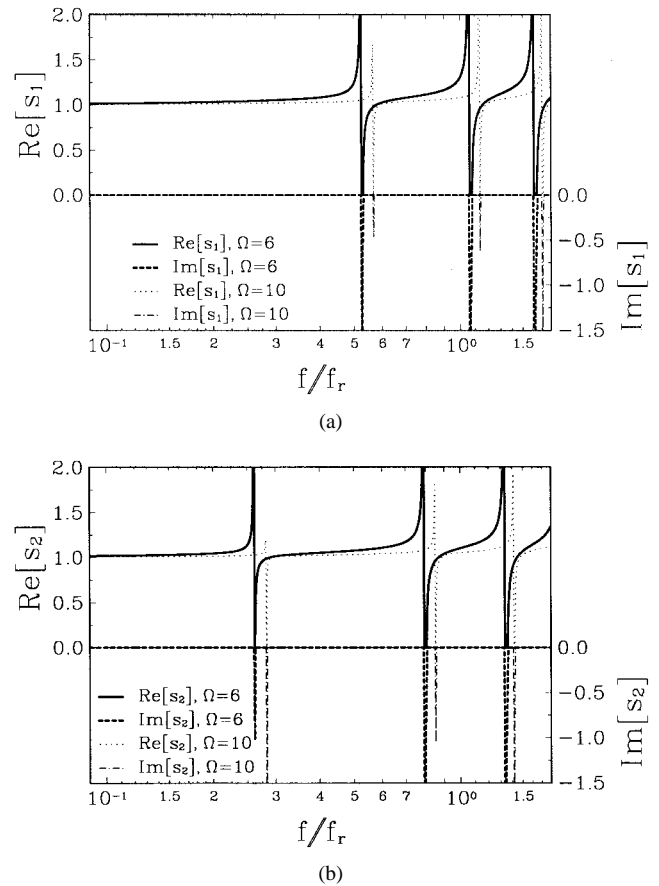

Fig. 7. Plots of normalized wavenumber $(s = k_z/k_o)$ as functions of relative frequency for $\Omega = 6$ and $\Omega = 10$. (a) The first root to the dispersion equation is displayed. (b) The second root. In both plots we account for the change in the dipole input impedance with frequency. The normalized transmission line length was fixed at $\Delta = L/\lambda_r = 1.5$. Additionally, for the purposes of plotting, we set $n\lambda_r^3 = 800$, $d = 0.1\lambda_r$, $\gamma = jk_o$, and $Z_o = 0.93\,\eta_o$. In each of these expressions, $\lambda_r = c_o/f_r$ is an arbitrary reference wavelength (a constant).

a given frequency, the wavenumbers are periodic functions of Δ. Thus, a medium composed of crossed-dipole inclusions with normalized line length $\Delta = n + x$ behaves (as far as the wavenumber is concerned) the same as one with normalized line length $\Delta = x$, where n is any integer.

Plots of normalized wavenumber as a function of relative frequency appear in Fig. 7; in these plots the normalized transmission line length is fixed. We notice that the resonances occur at different operating frequencies for the two different eigenstates. Fig. 8 shows the phase by which the y component of the electric field leads the x component for both polarization eigenstates. When the angle is $0°$ or $180°$, the polarization is linear (along the major axis of the degenerate polarization ellipse) and when the angle is $90°$ or $270°$ the polarization is circular. All other angles describe elliptically polarized waves. It is interesting to note that for certain ranges of Δ the argument of E_{oy}/E_{ox} is roughly a linear function of Δ. However, *near* the resonances $s_1\Delta$ (or $s_2\Delta$) becomes large and the phase $\arg[E_{oy}/E_{ox}]$ changes rapidly. Note that *within* the evanescence regions the two components of the electric field are either in phase or $180°$ out of phase, so in these regions the angle $\arg[E_{oy}/E_{ox}]$ is constant.
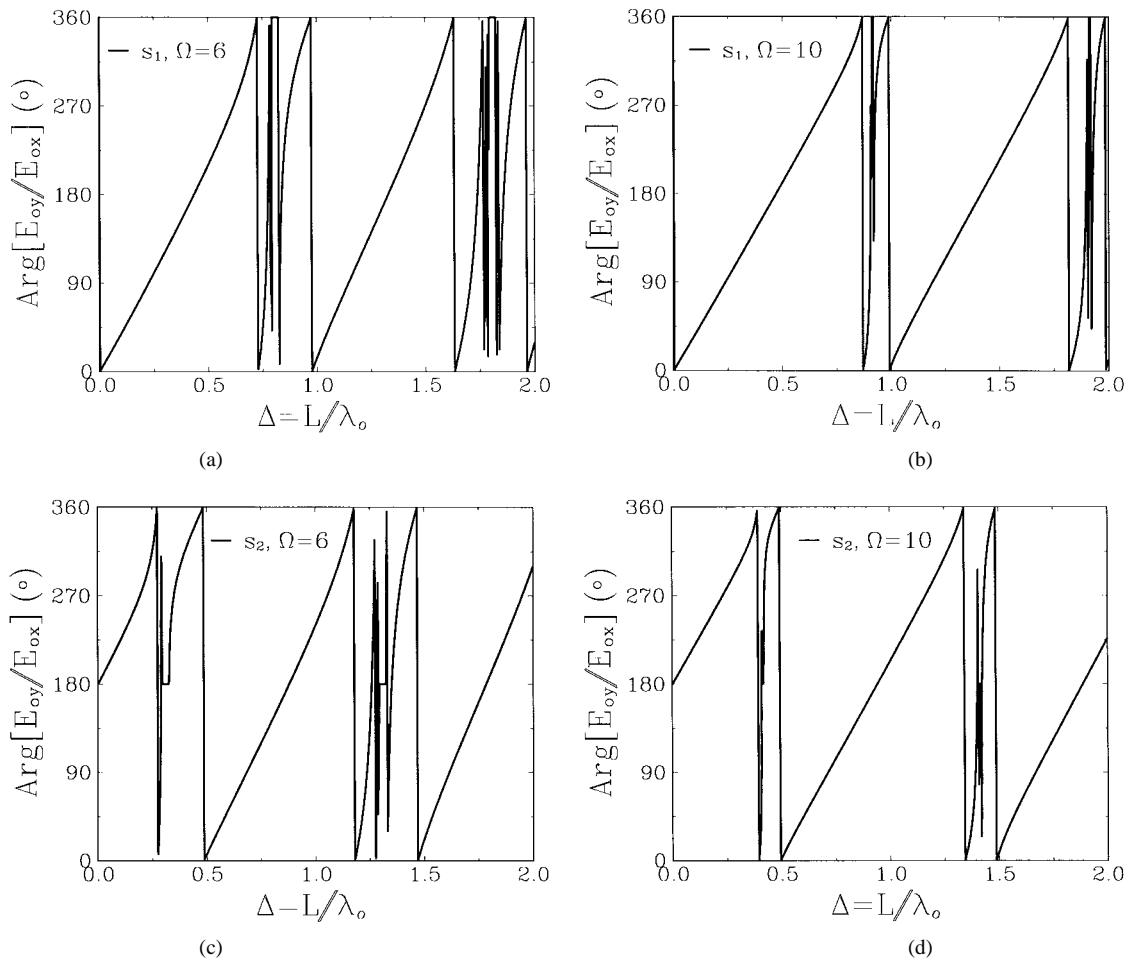
Fig. 8. The phase by which the y component of the electric field leads the x component for both wavenumbers when $\Omega = 6$ and $\Omega = 10$. (a), (b) The phase associated with the first root to the dispersion equation is displayed. (c), (d) The phase associated with the second root is displayed. In all four plots (as in Fig. 7) $n\lambda_o^3 = 800$, $d = 0.1\,\lambda_o$, $\gamma = jk_o$, $Z_o = 0.93\,\eta_o$, and we allow the transmission line length (L) to vary, keeping the operating frequency fixed.

Additionally, we point out an electromagnetic symmetry feature of crossed-dipole FFFB media. Namely, if an observer positions himself in the medium and *looks* toward $+z$ and then turns around to look toward $-z$, he would need to tilt his head 90° in order to see the same medium. In other words, if in (26) describing the polarization eigenstates one substitutes $-s_2$ $(-s_1)$ in place of s_1 (s_2) to denote propagation in the opposite direction, then the same set of waves is described only if the x and y axes are changed to y and $-x$, respectively.

V. SUMMARY

In this paper, we introduced one conceptualization of an artificial *feedforward–feedbackward* medium as an example of a material that seems to exhibit *macroscopic* feedback. As our particular example, we considered dipole–dipole FFFB media theoretically conceptualized by dispersing many dipoles throughout an isotropic host medium and linking pairs of these dipoles by parallel tiny transmission lines. The extra degree of freedom offered by the length of the link between the end inclusions of coupled-dipole FFFB media may offer interesting possibilities in the design of future microwave devices. One may speculate that by judiciously selecting the length of the connecting tiny transmission lines and thus modifying

the polarization eigenstates, novel polarizers—or polarization filters—could be realized. Such polarizers might find use in radomes and could be used to separate waves by polarization or by angle of refraction. Since we have shown that different eigenstates (for axial propagation) have different wavenumber, illumination of an interface separating a FFFB medium and a simple medium, with the interface oblique to the direction of the tiny transmission lines, would produce waves in the simple medium having a direction of propagation depending in part upon the wavenumber of the corresponding eigenstate in the FFFB medium.

Moreover, for the crossed-dipole case, we have shown that, in general, the permitted polarization eigenstates trace out counter-rotating ellipses, so, like chiral media, these media may have potential application as polarization rotators: by allowing a linearly polarized plane wave to illuminate a slab of crossed-dipole FFFB media, the wave emerging from the far-side of the slab may have different polarization from the incident wave. We have also found that the phase by which one component of the axial wave electric field leads the other component may, for certain ranges of parameters, be nearly a linear function of the normalized transmission line length for both polarization states (unlike, for example, chiral media, for which the polarization states are circularly polarized). This

property introduces the possibility of engineering a medium that permits certain desired polarization states at the far side of the slab given some specified incident wave.

Future directions for this work may include examination of oblique wave propagation in crossed-dipole FFFB media (taking into account the effects of direct interaction of the electromagnetic fields with the parallel tiny transmission lines), wave propagation in bounded FFFB media, and dyadic Green's functions in FFFB media. Although in this study we have focused on dipole–dipole FFFB media, other end inclusions can also be considered. One may, for instance, use a small loop, or a combination of a loop and a dipole, in place of each end dipole, thereby creating the possibility of constructing effectively bianisotropic artificial media. Work by other researchers (e.g., Saadoun and Engheta [21] and Auzanneau and Ziolkowski [34]) has already begun in this direction, so the future application of these types of media seems promising.

REFERENCES

[1] I. V. Lindell, A. H. Shivola, S. A. Tretyakov, and A. J. Vitanen, *Electromagnetic Waves in Chiral and Bi-Isotropic Media*. Boston, MA: Artech House, 1994.

[2] R. E. Collin, *Field Theory of Guided Waves*. New York: IEEE Press, 1991.

[3] W. E. Kock, "Metallic delay lenses," *Bell Syst. Tech. J.*, vol. 27, pp. 58–82, 1948.

[4] J. L. Blanchard, E. H. Newman, and M. E. Peters, "Integral equation analysis of artificial media," *IEEE Trans. Antennas Propagat.*, vol. 42, pp. 727–731, May 1994.

[5] J. Brown, "Artificial dielectrics having refractive indices less than unity," *Proc. Inst. Elect. Eng.*, vol. 100, pt. 4, pp. 51–62, May 1953.

[6] A. J. Bahr and K. R. Clausing, "An approximate model for artificial chiral material," *IEEE Trans. Antennas Propagat.*, vol. 42, pp. 1592–1599, Dec. 1994.

[7] D. L. Jaggard, A. R. Mickelson, and C. H. Papas, "On electromagnetic waves in chiral media," *Appl. Phys.*, vol. 18, pp. 211–216, 1979.

[8] J. Brown, "Artificial dielectrics," in *Progress in Dielectrics, Vol. 2*, J. B. Birks and J. H. Schulman, Eds. London, U.K.: Heywood, 1960, pp. 193–225.

[9] R. Luebbers, H. S. Langdon, F. Hunsberger, C. F. Bohren, and S. Yoshikawa, "Calculation and measurement of the effective chirality parameter of a composite chiral material over a wide frequency band," *IEEE Trans. Antennas Propagat.*, vol. 43, pp. 123–129, Feb. 1995.

[10] A. H. Shivola and L. V. Lindell, "Analysis on chiral mixtures," *J. Electromagn. Waves Applicat.*, vol. 6, no. 5/6, pp. 553–572, 1992.

[11] I. P. Theron and J. H. Cloete, "The optical activity of an artificial nonmagnetic uniaxial chiral crystal at microwave frequencies," *J. Electromagn. Waves Applicat.*, vol. 10, no. 4, pp. 539–561, 1996.

[12] S. A. Tretyakov and F. Mariotte, "Maxwell Garnett modeling of uniaxial chiral composites with bianisotropic inclusions," *J. Electromagn. Waves Applicat.*, vol. 9, no. 7/8, pp. 1011–1025, 1995.

[13] K. W. Whites, "Full-wave computation of constitutive parameters for loss-less composites chiral materials," *IEEE Trans. Antennas Propagat.*, vol. 43, pp. 376–384, Apr. 1995.

[14] F. Mariotte, S. A. Tretyakov, and B. Sauviac, "Modeling effective properties of chiral composites," *IEEE Antennas Propagat. Mag.*, vol. 38, pp. 22–32, Apr. 1996.

[15] S. A. Tretyakov, F. Mariotte, C. R. Simovski, T. G. Kharina, and J. Heliot, "Analytical antenna model for chiral scatterers: Comparison with numerical and experimental data," *IEEE Trans. Antennas Propagat.*, vol. 44, pp. 1006–1014, July 1996.

[16] S. I. Pekar, "The theory of electromagnetic waves in a crystal in which excitons are produced," *Soviet Phys., JETP*, vol. 6, no. 33, pp. 785–796, Apr. 1958.

[17] ——, *Crystal Optics and Additional Light Waves*. Menlo Park, CA: Benjamin/Cummings, 1983.

[18] R. Fuchs and P. Halevi, "Basic concepts and formalism of spatial dispersion," in *Spatial Dispersion in Solids and Plasmas*, P. Halevi, Ed. New York: North-Holland, 1992.

[19] L. B. Felsen and N. Marcuvitz, *Radiation and Scattering of Waves*. New York: IEEE Press, 1994.

[20] M. M. I. Saadoun and N. Engheta, "A reciprocal phase shifter using novel pseudochiral or Ω medium," *Microwave and Opt. Technol. Lett.*, vol. 5, pp. 184–187, 1992.

[21] ——, "Theoretical study of electromagnetic properties of nonlocal Ω media," in *Progress in Electromagnetic Research (PIER) Monograph Series Vol. 9 on Bianisotropic and Bi-Isotropic Media and Applications*, A. Priou, Ed. Cambridge, MA: EMW, 1994, ch. 15, pp. 351–397.

[22] C. Moses and N. Engheta, "Theoretical electromagnetic modeling of nonlocal-coupled-dipole artificial dielectric—Preliminary results," in *Symp. Dig. 14th Annu. Benjamin Franklin Symp. New Frontiers Antenna Microwave Technol.*, Philadelphia, PA, May 1996, pp. 92–93.

[23] S. N. Karp and F. C. Karal, Jr., "Excitation of surface waves on a unidirectionally conducting screen by a phased line source," *IEEE Trans. Antennas Propagat.*, vol. AP-12, pp. 470–478, July 1964.

[24] S. W. Schneider and B. A. Munk, "The scattering properties of "super dense" arrays of dipoles," *IEEE Trans. Antennas Propagat.*, vol. 42, pp. 463–472, Apr. 1994.

[25] R. W. P. King, *The Theory of Linear Antennas*. Cambridge, MA: Harvard Univ. Press, 1956.

[26] R. C. Johnson and H. Jasik, *Antenna Engineering Handbook*, chapter 4. New York: McGraw-Hill, 1984.

[27] R. W. P. King and T. T. Wu, "The cylindrical antenna with arbitrary driving point," *IEEE Trans. Antennas Propagat.*, vol. AP-13, pp. 710–718, Sept. 1965.

[28] W. L. Stutzman and G. A. Thiele, *Antenna Theory and Design*. New York: Wiley, 1981.

[29] R. W. P. King, *Arrays of Cylindrical Antennas*. Cambridge, MA: Cambridge Univ. Press, 1968.

[30] S. Silver, "Circuit relations, reciprocity theorems," in *Microwave Antenna Theory and Design*, S. Silver, Ed. London, U.K.: Peter Peregrinus Ltd., 1984.

[31] J. D. Jackson, *Classical Electrodynamics*. New York: Wiley, 1975.

[32] W. V. Tilston, T. Tralman, and S. M. Khanna, "A polarization selective surface for circular polarization," in *IEEE AP-S Int. Symp.*, Syracuse, NY, June 1988, vol. II, pp. 762–765.

[33] J. E. Roy and L. Shafai, "Reciprocal circular polarization selective surfaces," *IEEE Antennas Propagat. Mag.*, vol. 38, pp. 18–33, Dec. 1996.

[34] F. Auzanneau and R. W. Ziolowski, "Theoretical study of synthetic bianisotropic materials," *J. Electromagn. Waves Applicat.*, vol. 12, no. 3, pp. 353–370, 1998.

Charles A. Moses (S'92–M'97), received the B.S.E.E. and M.S.E.E. degrees from the Virginia Polytechnic Institute and State University, Blacksburg, in 1992 and 1993, respectively, and the Ph.D. degree from the University of Pennsylvania, Philadelphia, in 1997.

Since 1997, he has been with the U.S. Government, Washington, DC. His current work is in the area of theoretical and applied electromagnetics, with a special interest in wave propagation, complex media, nonlinear microwave circuits, and innovative antennas.

Dr. Moses recently won second place at the 1998 URSI Radio Science Student Paper Competition, Boulder, CO. He is a member of Tau Beta Pi, Eta Kappa Nu, and Phi Kappa Phi.

Nader Engheta (S'81–M'82–SM'89–F'96), for a photograph and biography, see p. 566 of the April 1996 issue of this TRANSACTIONS.